JOURNAL OF MATERIALS SCIENCE **36** (2001) 3925–3931

Study of BCN compounds prepared by the chemical vapor deposition with dimethylamineborane

MASAHIRO MIENO, TADAO SATOH
Advanced Materials Laboratory, National Institute for Materials Science, 1-1 Namiki Tsukuba, Ibaraki 3050044, Japan

B-C-N films were synthesized by using the chemical vapor deposition in which the starting material dimethylamineborane was transported onto a substrate with nitrogen gas, and analyzed with secondary electron microscopy, Raman scattering, infrared spectroscopy, x-ray photoelectron spectroscopy, transmission electron microscopy, electron diffraction, x-ray diffraction, and ultraviolet-visible-rays absorption spectroscopy. Effects of substrate temperature and deposition pressure on the solid-solutions of B-C-N films were investigated by changing substrate temperature between 700 and 1000 °C under deposition pressure between 100 and 760 Torr. It was found that a mixture of microcrystal glassy carbon and turbostratic-BN both with an apparent crystal size of about 10 Å was deposited under the atmospheric pressure at 1000 °C. In deposition where the pressure was reduced from the atmospheric pressure to 600 Torr, BN gradually lost the stoichiometric compositions to form a mixed structure of BNx ($x < 1$) and glassy carbon. In deposition where the pressure was lowered than 600 Torr, BNxCy : H (x,$y < 1$) of which dangling bonds were terminated with hydrogen was produced as a result of further decrease of the BNx nitriding rate and then substitution of carbon for nitrogen. This BNxCy : H (x,$y < 1$) showed character close to amorphous material and the composition ratio varied continuously for the deposition pressure change.

1. Introduction

BN and C have analogous polymorph and phase diagram. In addition, each of the polymorph shows excellent properties in heat resistance, corrosive resistance, hardness, etc. From these facts, it has been expected that a BCN ternary compound may exist as an intermediate compound of BN and C showing both of the excellent properties or complementing their defects mutually [1], their syntheses have been attempted [2–4] and various intermediate compounds have been reported [5–12]. Recently, a report about the existence of BC_2N has been published [13], leading to syntheses and analyses of the compound and calculations regarding the phase stability [14, 15]. Based on those studies, in this research, it was tried to synthesize BCN ternary compounds by using the chemical vapor deposition (CVD) in which the dimethylamineborane was used as the starting material having the same composition ratio as BC_2N, with regard to B, C, and N, and comprehensive analysis was performed using secondary electron microscopy (SEM), transmission electron microscopy (TEM), x-ray diffraction (XRD), infrared spectroscopy (IR), Raman scattering, x-ray photoelectron spectroscopy (XPS), etc., in order to identify its solid-solution relating to synthesis conditions.

2. Experimental method

Dimethylamineborane melts at the temperature of 36 °C, and begins to decompose and evaporate gradually. At above 70 °C, dimethylamineborane changes into dimethylaminoborane due to its own dehydrogenation reaction. Therefore, dimethylamineborane was kept at 60 °C in evaporator and fed with career gas in order to allow deposition to occur with supply of sufficient vapor pressure and without the decomposition. The vapor pressure of dimethylamineborane at 60 °C is approximately 1.5 mmHg. Fig. 1 is a schematic diagram of the CVD equipment used in this experiment. In order to allow starting material to reach the substrate without decomposition, a evaporator was placed just under the substrate and a gas feeder was cooled to prevent temperature increase due to radiation heat from the substrate. Moreover, career gas was purified of oxygen and water through columns and injected in to the evaporator, and then passed on the liquid surface of dimethylamineborane at a constant rate so that the initial material was steadily transported. The deposition procedure was as follows. The chamber was exhausted to less than 10^{-7} Torr with a turbo pump; the substrate was heated up to 1000 °C for degasification; nitrogen gas was filled in the chamber up to the deposition pressure; the substrate and the evaporator were heated up

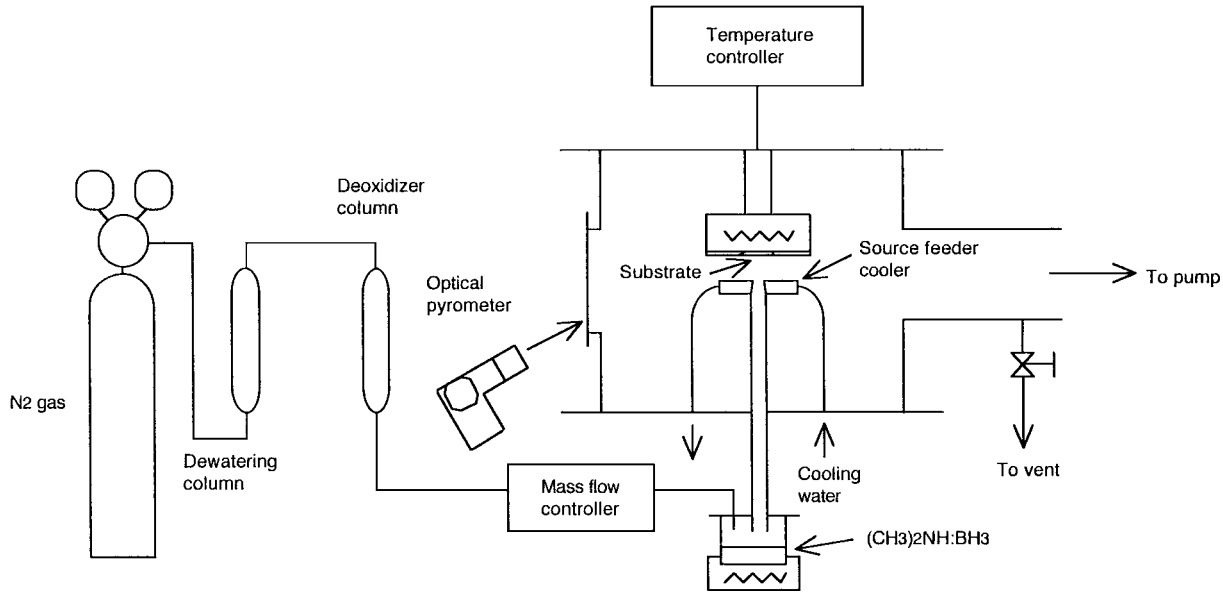

Figure 1 Schematic diagram of the CVD apparatus.

to the desired temperature; then nitrogen of the career gas was flowed to produce deposition at 400 sccm. As the supplement of the starting material was kept constant, the nitrogen partial pressure decreased with decreasing the deposition pressure. Deposition was produced changing substrate temperature between 700 and 1000 °C for every deposition pressure between 100 and 760 Torr to examine the effects of substrate temperature and deposition pressure. In addition, one of Si (111), quartz, Ni, and Mo was chosen for the substrate according to analytical method or to see effects of the substrate in the deposition.

Each obtained product was analyzed by using all of SEM, TEM, XRD, transmission electron diffraction (TED), Raman scattering, IR, ultraviolet-visible-rays absorption spectroscopy, and XPS.

3. Results and discussions

3.1. Configuration observation

Deposits were all flat and smooth films, each of which color changed variously from transparent yellow through glossy dark brown with an increase in deposiston temperature. It had also been observed that adhesion differed depending on substrates. To Si and quartz substrate, films were adhered, but to the latter, films deposited under 100 to 300 Torr were exfoliated partially. To metal substrate such as Ni, Mo, films deposited in any condition were peeled. A typical SEM image of the deposited films is shown in Fig. 2. As shown in the cross section of Fig. 2a, the films were dense and did not show layer structure characteristic of pyrolytic boron nitride (PBN) and pyrolytic graphite (PG). As shown in Fig. 2b, pelletized structure with spacing of several tenth of nano meters was observed on the surface. This configuration did not change regardless of the kind of substrate material, also deposition rate and substrate temperature.

3.2. XRD, TED, and TEM

Structure analysis was performed using XRD and TED. Fig. 3 shows a typical XRD pattern. The films showed

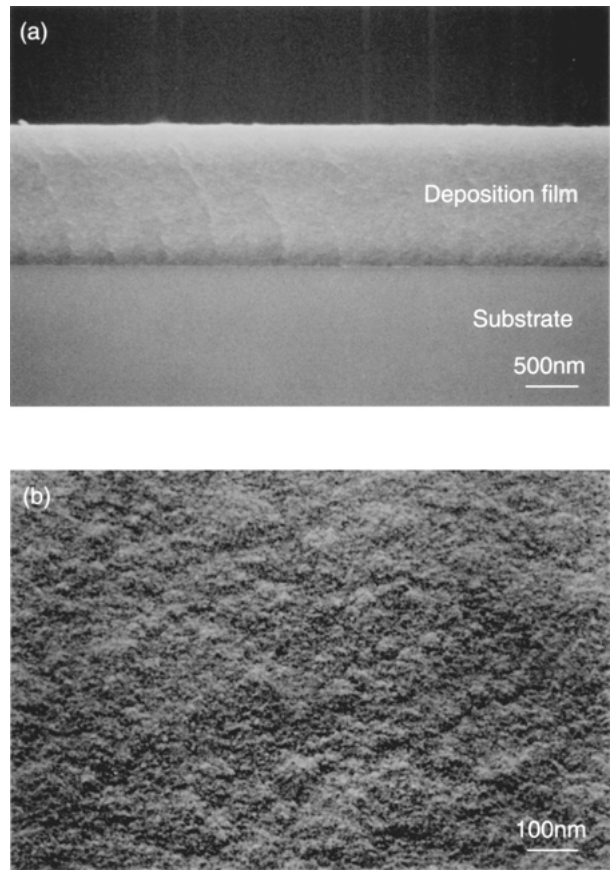

Figure 2 Typical (a) sectional view photograph and (b) surface view photograph of deposited films taken by a scanning electron microscope.

a typical turbostratic pattern [16] with only diffraction peaks from (00l) and (hk0) of the graphite structure. This means that the structure of films had basically hexagonal network and random-layer caused by sliding of stacking layers. Moreover, the apparent crystal sizes in the direction of a-axis and c-axis, *La* and *Lc*, of graphite structure were respectively given as 16 and 10 Å by the Scherrer formula, and their changes were only within ±10% even if the substrate temperature and other experiment conditions were changed. As seen in

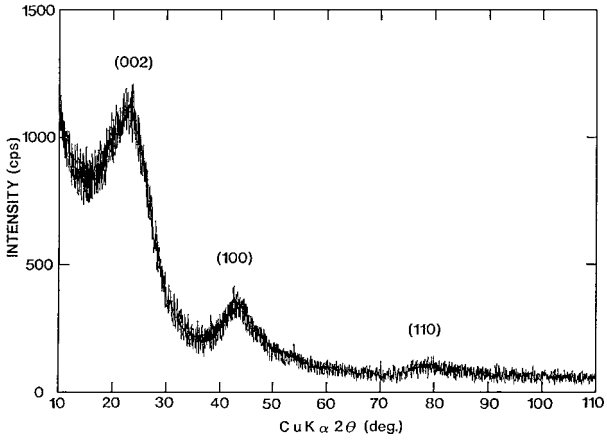

Figure 3 Typical X-rays diffraction pattern of deposited films.

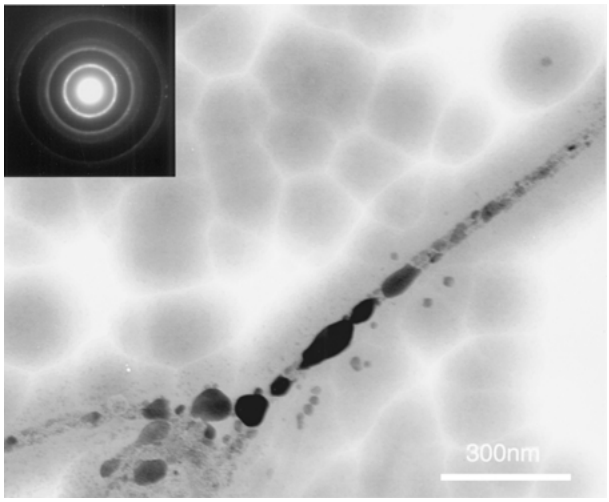

Figure 4 Transmission electron diffraction pattern and microscopic image of a film deposited under a reduced pressure.

Fig. 4, electron diffraction of typical sample showed a halo ring pattern, which was characteristic of microcrystal structure. Table I is a list of the d(Å) value and its relative intensity of this sample with those of ASTM data of hexagonal-BN (h-BN) and carbon. Similarly to the XRD case, only (hk0) and (00l), but no three-dimensional diffraction were observed. Longer lattice spacings of (00l) compared with ASTM data were observed and the extension of interlayer spacings was characteristic of turbostratic. The lattice spacings of (hk0) was slightly close to that of the h-BN compared with carbon. Since there was no large difference between the relative strengths of the XRD and TED with different direction of incident beam to film growth direction, no deposition occurred in preferred orientation in contrast with PBN and PG growth along c-axis orientation.

TABLE I The measured lattice spacings of each reflection compared with ASTM

Observed Value		ASTM 9-12 (h-BN)			ASTM 23-64 (Carbon)		
d (Å)	I/Io	d (Å)	I/Io	hkl	d (Å)	I/Io	hkl
3.53	vs	3.33	100	002	3.36	100	002
2.17	s	2.17	16	100	2.13	10	100
		2.06	6	101	2.03	50	101
		1.817	14	102	1.800	5	102
1.73	w	1.667	6	004	1.678	80	004
		1.552	2	103	1.544	10	103
		1.322	4	104			
1.25	w	1.253	6	110	1.232	30	110
		1.173	8	112	1.158	50	112
		1.111	2	006	1.120	20	006
		1.086	2	200	1.054	5	201
		1.032	2	202			
		1.001	6	114	0.994	40	114
		0.989	2	106			106
		0.910	2	204			
		0.83	6	008	0.841	10	008

The TEM image of a sample deposited under the atmospheric pressure showed homogeneous structure with flat contrast. However, as shown in Fig. 4, a sample synthesized under a reduced pressure showed high and low contrast parts, the latter of which composed of condensation of fine bubbles. The rate of the low contrast parts tended to increase as deposition pressure was reduced. By comparison of the two parts brightness, it considered that the former had microcrystal structure and the latter was composed of an amorphous component.

3.3. Raman scattering, IR, and ultraviolet-visible-rays absorption spectroscopy

Fig. 5 shows a typical Raman scattering spectrum for deposited films. All the measurements were performed in the back-scattering arrangement, where an Ar-laser 5145 Å beam was mainly used as excitation rays and a 4880 Å beam was also used for confirmation, if necessary. The spectrum shown in the figure was similar to that of glassy carbon (GC), which consisted of two broad peaks, the one so-called disordered(D)-peak in the vicinity of 1350 cm^{-1} [17], and the other graphitic(G)-peak due to the E_{2g} mode of graphite in the vicinity of 1590 cm^{-1} [18]. The reason for D-peak occurrence is that crystalline disorder alleviates the $\boldsymbol{q} \sim 0$ Raman selection rules so that phonons throughout the Brillouin zone are activated. Near the D-peak, there exists Raman peak around 1360 cm^{-1} [19] due to the E_{2g} mode of the h-BN, but it had never been observed being clearly separated from the broad band in the vicinity of 1350 cm^{-1}. However, some samples showed peak-like behavior at 1380 cm^{-1} as shown in the figure. The peak corresponding to the E_{2g} mode of

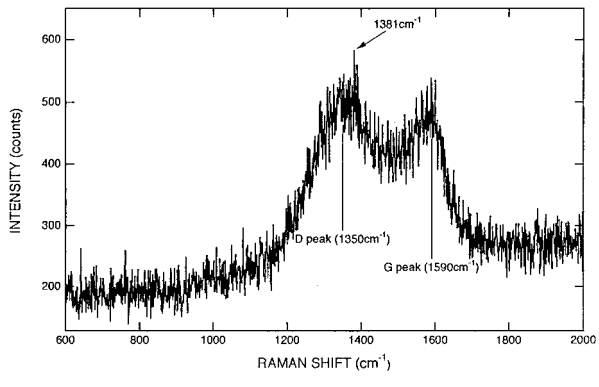

Figure 5 Typical Raman spectrum of deposited films.

h-BN is observed maximally at 1360 cm^{-1} for highly ordered crystal, with the Shear mode in the vicinity of 50 cm^{-1} [19, 20]. If it is turbostratic, the Shear mode at 50 cm^{-1} disappears and the E_{2g} mode at 1360 cm^{-1} shifts to the high wave number around 1380 cm^{-1}, where the scattering intensity decreases by 2 or 3 orders with the decrease of apparent crystal size. The scattering intensity observed in BCN films was normally the same level as that of turbostratic-BN (t-BN) having the apparent crystal size of 1000 Å. Considering that apparent crystal size of the deposited films obtained in this experiment was at most several 10 Å, it might be difficult to measure the t-BN peak separately from D-peak even if t-BN existed. Therefore, it can be said that no observation of the E_{2g} mode of h-BN does not mean non-existence of BN. Moreover, other peaks were not observed in any samples where measurements were performed with Raman scattering in a region between 30 and 4000 cm^{-1}, showing no evidence of other materials such as B_4C.

Fig. 6 shows a typical behavior of IR spectra when deposition temperature was varied. Deposited sample on single-crystal Si substrate was used in the IR measurament. The deposited films showed peaks in the vicinity of 1380 and 800 cm^{-1}, each of which corresponds to the wave number of stretching (E_{1u}) and bending (A_{2u}) vibrations of h-BN [20], respectively. As substrate temperature was lowered in deposition, a peak considered to correspond to stretching vibration of the hexagonal network shifted to the lower wave-number side of 1380 cm^{-1} and a peak considered to correspond to bending vibration also shifted to the lower wave-number side and the width tended to spread further. Fig. 7 is a summary of peak behavior in the vicinity of 1380 cm^{-1} when pressure and deposition temperature were varied. When deposition was performed under conditions of substrate temperature of 1000 °C and atmospheric pressure, a peak appeared at 1380 cm^{-1}. As substrate temperature was lowered, the peak tended

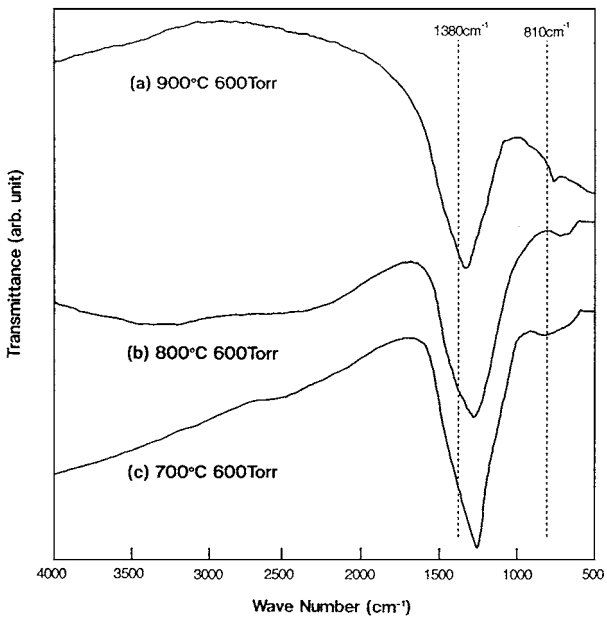

Figure 6 IR spectrum behavior of deposited films against deposition temperature change.

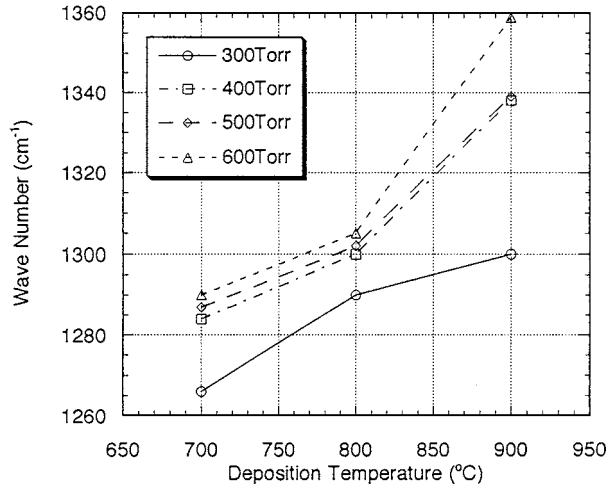

Figure 7 Wave number change corresponding to stretching vibration of BN against deposition temperature and pressure.

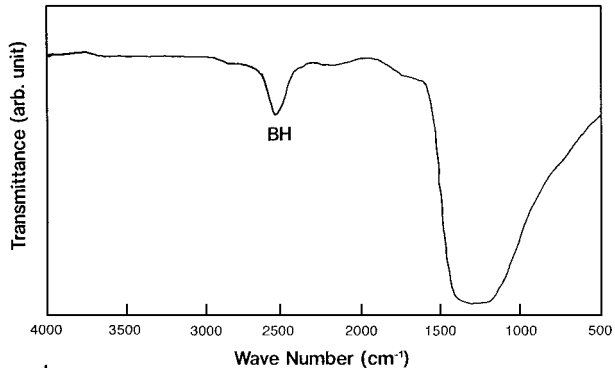

Figure 8 Typical IR spectrum of films deposited under reduced pressure.

to shift almost linearly to the lower wave-number side. As deposition pressure was lowered, the wave number of the peaks also tended to decrease. As shown in Fig. 8, sample deposited at 400 Torr or below revealed an observable peak at 2500 cm^{-1} that corresponded to stretching vibration of BH, where bending vibration mode of hexagonal network could not be identified because of broadening width of stretching vibration mode. In addition, absorption peaks of CH, NH, CN, etc. were not observed in all samples.

Furthermore, absorption spectroscopy was conducted in a range of ultraviolet-visible rays by using samples deposited on quartz substrates. As deposition temperature increased, in absorption spectroscopy, the absorption edge in the ultraviolet-visible-rays range tended to shift to the long wave length side and the transmittance in the visible range decreases from 95% (600 °C) to 55% (1000 °C). The band gap estimated from the absorption edge was 4.8 eV at a deposition temperature of 600 °C. It decreased with the increase of the deposition temperature and became 2.5 eV at 1000 °C. On the other hand, the absorption edge did not move when deposition pressure had been varied at a fixed temperature,

3.4. XPS analysis

In order to detect constituent elements and determine the composition ratio, XPS was performed using photoelectron spectra in the range of 0 to 1000 eV with MgKα

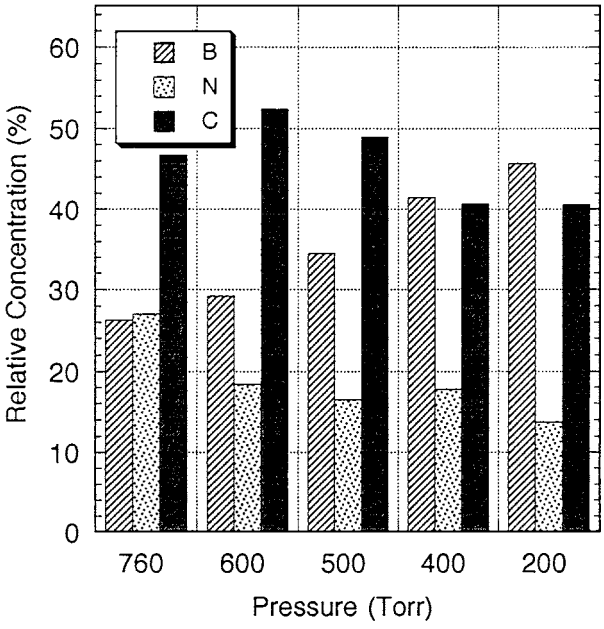

Figure 9 Relative concentration behavior of B, C, and N of deposited films against deposition pressure change at a fixed deposition temperature of 900 °C.

(1253.6 eV) as an excitation source. Bonding of B, C, and N was studied from the XPS spectra of B1s, C1s, and N1s.

First, in the spectrum of 0 to 1000 eV, O was observed as an impurity other than peaks of B, C, and N. The atomic composition ratio was determined by dividing the area of each peak by the sensitivity coefficient. A concentration of impurity oxygen was always approximately 2 or 3%. Fig. 9 shows relative concentration behavior of B, C, and N against the working pressure for deposition temperature of 900 °C. For fixed pressure, the composition ratio only changed within 5% in a range of deposition temperature between 600 and 1000 °C showing no tendency specific to temperature variation. When deposition had been produced under the atmospheric pressure, the ratio of B to N took substantially 1:1 and C was 1.8 times as much as B and N. As deposition pressure decreased, the ratio of N to B and also that of C to B decreased, which resulted in lower relative ratio of C than B at working pressure of 400 Torr or below. The composition ratio changed continuously against deposition pressure variation, and it was not observed that a composition ratio was stable.

Fig. 10 showed XPS spectra for B1s, N1s, and C1s against deposition pressure variation, respectively. The binding energy of B1s was 190.7 eV for deposits obtained under the atmospheric pressure. The energy shifted to the lower energy side with the decrease of the deposition pressure, reaching a value of 188.3 eV at 200 Torr, as the spectrum showed a single symmetrical peak. On the other hand, N1s spectrum having a single symmetrical peak at 398.3 eV did not show any change when deposition pressure was decreased. Although C1s shows a single symmetrical peak at 284.5 eV for deposits under the atmospheric pressure, decrease of deposition pressure caused peaks on the

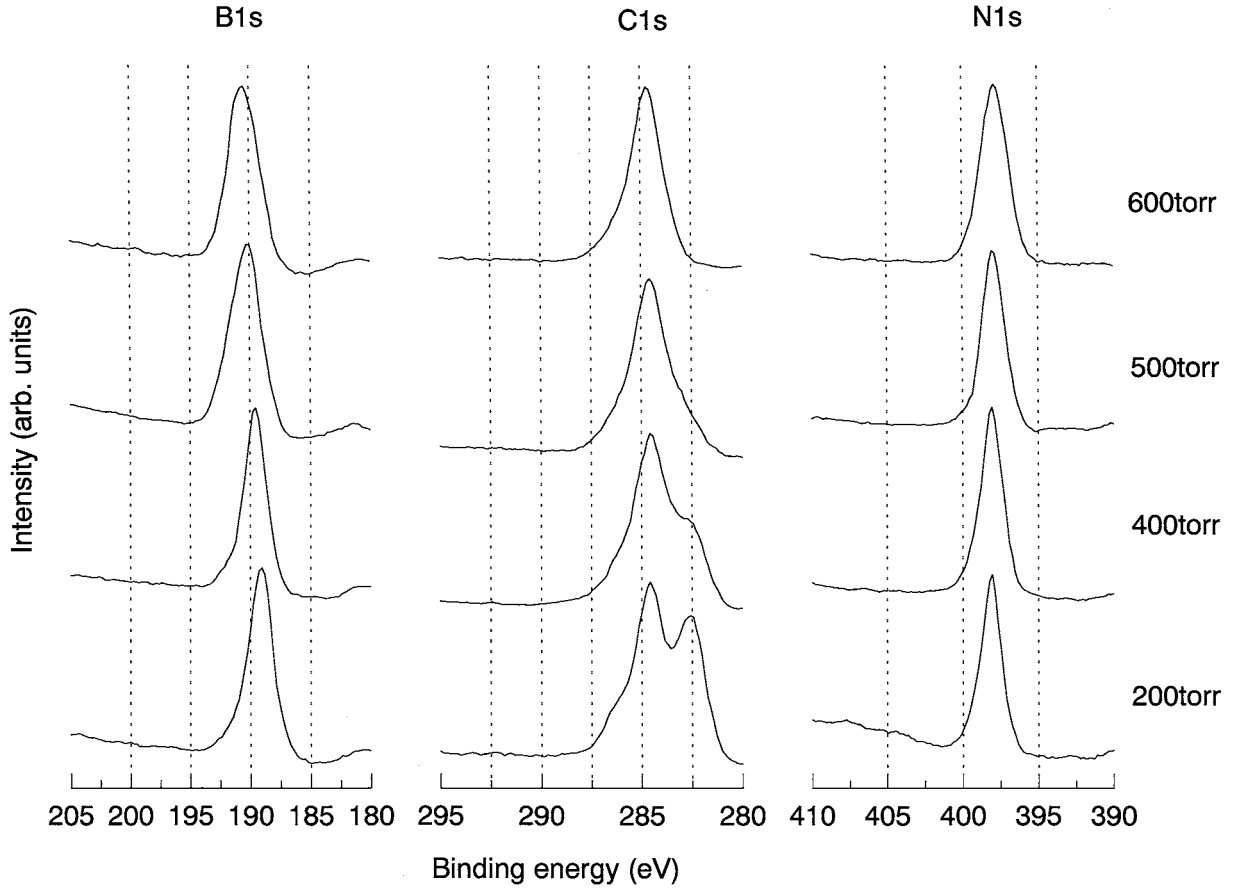

Figure 10 B1s, C1s, and N1s photoelectron spectra behavior of deposited films against deposition pressure change at a fixed deposition temperature of 1000 °C.

TABLE II Core-electron binding energies of each element of the main compounds composed of B, C, and N

	Boron	Carbon	Nitrogen	Oxygen
Metal B [21]	187.5			
BN [22]	190.6		398.3	
B_2O_3 [22]	193.4			533.0
B_4C [23]	186.6	281.8		
C(graphite) [24]		284.3		
CH_3CN [25]		287.4	399.6	

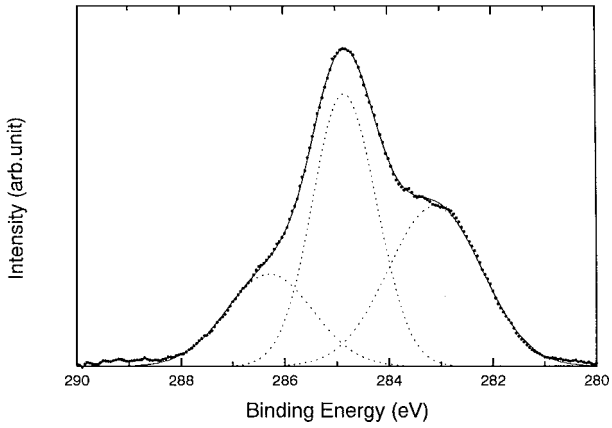

Figure 11 Gaussian curve fitting of C1s spectrum of film deposited at 400 Torr.

lower and higher energy sides other than the primary peak at 284.5 eV. Fig. 11 show the result of C1s peaks separation performed by means of Gaussian curve fitting of $BN_{0.43}C_{0.97}$ deposited at pressure of 400 Torr. The peak on the lower energy side than the primary peak was at 283.1 eV and occupied 37% of the whole C1s spectrum area. The peak on the higher energy side was at 286.3 eV and occupied 20% thereof. As deposition pressure decreased, the positions of two satellite peaks relative to the primary peak did not move and their area ratios to the primary peak tended to increase.

Table II is a list of binding energies of main compounds in the B-C-N system. Since chemical shift of B1s takes +3.1 eV and +5.9 eV for nitride and oxide respectively compared with 187.5 eV for metal B, it is understood that the binding energy depends on ionic bond strength. Since B_4C is formed as covalent bond, B1s and C1s shift to the lower energy side by −0.9 V and −2.5 eV respectively for both metal B and graphite. When C combines with N, C1s shifts to the higher energy side by +3.1 eV.

Referring to these facts, sample deposited under pressure between the atmospheric pressure and 600 Torr considered to be composed of BN and C, since the chemical shift values of B1s and N1s coincided with BN and the value of C1s also with graphite.

As deposition pressure decreased, however, the chemical shift of B1s decreased and approached the value of metal B, and that of N1s did not change. This is considered as follows. The nitrogen partial pressure decreases while keeping the supplement of the starting material as the total pressure reduces; as shown in Fig. 9, decrease tendency of the ratio of N to B indicates that insufficient nitriding reaction causes nitrogen defect in BN; then that dangling bonds produced thereby in BN displace with C or B to reduce the chemical shift of the B1s peak. When BN was produced with the sputtering method, the B1s peak separated into peaks of BN and metal B due to decrease of nitriding rate [26]. This is because the reaction system contains only inert gas other than B and N, which differs from this experiment, and the reaction advances separation into BN and metal B rather than lattice defect formation, resulting in peak separation in B1s spectrum. In this experimental system, however, only the chemical shift of B1s decreased and peak separation was not seen since displacement with surrounding C and H surpassed separation into BN and metal B in the reaction. On the other hand, the change of C1s spectrum with the decrease of deposition pressure is interpreted as follows. Since C substitute N in the BN hexagonal network and combine with B, C1s gave a peak shifted by −1.7 eV other than the graphite peak. The substitution of C in the BN hexagonal network make it unstable to repeat the structure periodically and lead it to the amorphous state. As the result, there occurs a state where N and C atoms become coadjacent besides B-C and B-N showing a weak peak at +3.2 eV on the higher energy side.

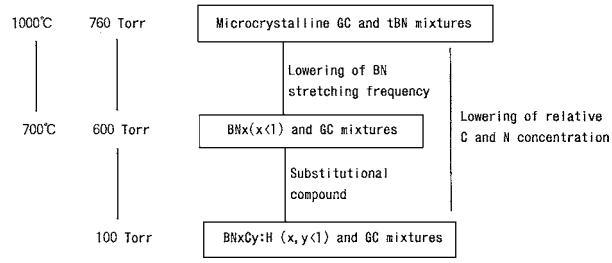

Figure 12 Reaction process change of dimethylamineborane against deposition temperature and pressure.

4. Summary and conclusion

Fig. 12 is a summary of experimental results obtained with the CVD with dimethylamineborane by varying deposition temperature and pressure. When deposition was produced at the temperature of 1000 °C under the atmospheric pressure, dimethylamineborane underwent decomposition reaction separating into stable GC and t-BN. As a result, the deposited films showed the turbostratic pattern in XRD and TED, the spectrum pattern of BN in IR, that of GC in Raman scattering, and the binding energy of BN and graphite in XPS analysis. When deposition was performed by decreasing substrate temperature from 1000 °C, calcination of BN and carbon became insufficient. Because of this, the peak corresponding to the BN stretching vibration mode shifted to the lower wave number side as seen in the IR spectrum, and the optical absorption edge shifted to the higher energy side. When deposition was conducted by reducing pressure within the range of up to 600 Torr, BN lost the stoichiometric composition and then the films deposited exhibiting a mixed structure of BNx ($x < 1$) and GC. When deposition was conducted by reducing the pressure further, the nitriding rate decreased causing C displacement in BN and the films became a mixture of

GC and BNxCy : H(x, $y < 1$) of which dangling bonds were terminated with H. This BNxCy : H(x, $y < 1$) was considered to be close to amorphous rather than turbostratic microcrystal. This interpretation is based on a fact that BN stretching vibration spectrum was broaden in IR, and a portion having a low contrast was separately observed in TEM images. These character changes of the films occurred continuously against deposition pressure variation and there was no behavior observed that indicated existence of fixed composition.

As descried above, if quantity of surrounding nitrogen is enough to nitride dimethylamineborane, B attempts to couple with N to organize hexagonal network, and to separate from C. However, if surrounding nitrogen decreases, nitriding of BN becomes insufficient and B catches C, and H terminates dangling bonds. The residual C that cannot combine with B or N forms graphite. In other words, if dimethylamineborane polymerizes by suppressing nitriding and calcination, bonding in the starting material is remained and BNC compounds are produced. However, these compounds are not in stable phases since they show continuous changes in composition depending on variation of experimental conditions.

References

1. TAKAYOSHI SASAKI and YOSHINORI FUIKI, *Gypsum & Lime* **219** (1989) 45.
2. A. W. MOORE, S. L. STRONG, G. L. DOLL, M. S. DRESSELHAUS, I. L. SPAIN, C. W. BOWERS, J. P. ISSI and L. PIRAUX, *J. Appl. Phys.* **65**(12) (1989) 15.
3. LEON MAYA and LAWRENCE A. HARRIS, *J. Am. Ceram. Soc.* **73** (1990) 1912.
4. MASAO YAMADA, MASAFUMI NAKAISHI and KENJI SUGISHIMA, *J. Electrochem. Soc.* **137**(7) (1990) 2242.
5. T. YA. KOSOLAPOKA, G. N. MAKARENKO, T. I. SEREBRYAKOVA, E. V. PRILUTSKII, O. T. KHORPHYAKOV and O. I. CHERNYSHEVA, *Pooshkovaya Metallurgiya* **1** (1971) 27.
6. ANDRZEJ R. BADZIAN, *Mat. Res. Bull.* **16** (1981) 1385.
7. K. MONTASSER and S. HATTORI, *Thin Solid Films* **117** (1984) 311.
8. T. V. DUBOVIK and T. V. ANDREEVA, *J. Less-Common. Metals* **117** (1986) 265.
9. R. B. KANER, J. KOUVETAKIS, C. E. WARBLE, M. L. SATTLER and N. BARTLETT, *Mat. Res. Bull.* **22** (1987) 399.
10. T. M. BESMANN, *J. Am. Ceram. Soc.* **73** (1990) 2498.
11. JOACHIM BILL and RALF RIEDEL, *Mat. Res. Soc. Symp. Proc.* **271** (1992) 839.
12. FREDERIC SAUGNAC, FRANCIS TEYSANDIER and ANDRE MARCHAND, *J. Am. Ceram. Soc.* **75** (1992) 161.
13. J. KOUVETAKIS, T. SASAKI, C. SHEN, R. HAGIWARA, M. LERNER, K. M. KRISHNAN and N. BARTLETT, *Synth. Metals.* **34** (1989) 1.
14. WALTER R. L. LAMBRECHT and BENJAMIN SEGALL, *Phys. Rev. B* **47** (15) (1993) 47.
15. H. NOZAKI and S. ITOH, *J. Phys. Chem. Solids* **57** (1996) 41.
16. J. THOMAS JR., N. E. WESTON and T. E. O'CONNOR, *J. Am. Chem. Soc.* **84** (1963) 4619.
17. J. H. KAUFMAN and S. METIN, *Phys. Rev. B* **39**(18) (1989) 39.
18. F. TUINSTRA and J. L. KOEING, *J. Chem. Phys.* **53**(3) (1970) 1126.
19. R. J. NEMANICH and S. A. SOLIN, *Bull. Am. Phys. Soc.* **20** (1975) 429.
20. R. GEICK, C. H. PERRY and G. RUPPRECHT, *Phys. Rev.* **146** (1966) 543.
21. D. H. HENDRICKSON, J. M. HOLLANDER and W. L. JOLLY, *Inorganic Chemistry* **9**(3) (1970) 612.
22. DAVID J. JOYNER and DAVID M. HERCULES, *J. Chem. Phys.* **72**(2) (1980) 1095.
23. C. VINCENT, H. VINCENT, H. MOURICHOUX and J. BOUIX, *J. Mat. Sci.* **27** (1992) 1892.
24. K. L. SMITH and K. M. BLACK, *J. Vac. Sci. Technol. A* (2) (1984) 744.
25. M. BARBER, J. A. CONNER, M. F. GUEST, I. H. HILLER, M. SCHWARZ and M. STACEY, *J. Chem. Soc. Faraday Trans.II* **69** (1973) 551.
26. M. MIENO and Y. TOSHIDA, *Surface and Coatings Technology* **52** (1992) 87.

Received 27 June 2000
and accepted 21 March 2001